PAPER

Check for updates

Characterization of plasma polymerized acetonitrile film for fluorescence enhancement and its application to aptamer-based sandwich assay

Kazuyoshi Yano, [ID] *[a] Yutaro Matsuie,[a] Ayaka Sato,[b] Maiko Okada,[a] Takuo Akimoto[a] and Iwao Sugimoto[c]

Among biosensing systems for sensitive diagnoses fluorescence enhancement techniques have attracted considerable attention. This study constructed a simple multilayered structure comprising a plane metal mirror coated with a plasma-polymerized film (PPF) as an optical interference layer on a glass slide for fluorescence enhancement. Plasma polymerization enables the easy deposition of organic thin films containing functional groups, such as amino groups. This study prepared PPFs using acetonitrile as a monomer, and the influences of washing and the output powers of plasma polymerization on PPF thickness were examined by Fourier transform infrared spectroscopy. This is because controlling the PPF thickness is vital in fluorescence enhancement. Multilayered glass slides prepared using a silver layer with 84 nm-thick acetonitrile PPFs exhibited 11- and 281-fold fluorescence enhancements compared with those obtained from the substrates with a bare surface and only modified by the silver layer, respectively. Oligonucleotides labeled with a thiol group and cyanine5 were successfully immobilized on the multilayered substrates, and the fluorescence of the acetonitrile PPFs was superior to that of the allylamine and cyclopropylamine PPFs. Furthermore, an aptamer-based sandwich assay targeting thrombin was performed on the multilayered glass slides, resulting in an approximately 5.1-fold fluorescence enhancement compared with that obtained from the substrate with a bare surface. Calibration curves revealed the relationship between fluorescence intensity and thrombin concentration of 10–1000 nM. This study demonstrates that PPFs can function as materials for fluorescence enhancement, immobilization for biomaterials, and aptamer-based sandwich assays.

1. Introduction

Fluorescence-based detection is widely employed for various biomedical diagnostic applications. To enhance diagnosis (particularly at preliminary stages), certain strategies have been reported to improve the fluorescence sensitivity and low limit of detection (LOD) of biomarkers. These strategies include ZnO nanostructure-modified microfluidic devices,[1] phosphate-triggered fluorescence turn-on detection,[2] CRISPR/Cas13a-based signal amplification[3] and ratiometric fluorometry triggered by alkaline phosphatase.[4] Among them, metal-enhanced fluorescence (MEF) is a powerful technology that significantly enhances fluorescence signals and shields fluorophores against the photo-bleaching process.[5,6] MEF is an optical phenomenon induced by localized surface plasmon resonance, where the

fluorescence intensity can be considerably enhanced by placing noble metal nanostructures and fluorophores in proximity. Owing to its outstanding potential, MEF has been applied to highly sensitive C-reactive protein immunoassays,[7] silver plasmonic microarray substrates,[8] two-dimensional (2D) periodic nanopatterned arrays[9] and simple-to-use detection by entrapping gold nanoparticles in nitrocellulose membranes.[10] Furthermore, highly sensitive miRNA detection has been achieved using ultraflat-faceted core–shell nanocuboids with >1000-fold sensitivity compared with conventional assays.[11]

Another promising tool for fluorescence enhancement is a simple multilayered structure comprising a plane metal mirror coated with an optical interference layer on a glass slide. Waveguide mode enhancement was first reported and further examined by Hall's group. They reported that the fluorescence intensity of rhodamine B was enhanced by more than two orders of magnitude using a multilayered substrate fabricated with the dielectric LiF as an optical interference layer on the surface of a silver mirror.[12–15] The enhancement effect was highly dependent on the thickness of the optical interference layer, and peaks of fluorescence intensity as a function of the layer thickness were periodically observed. The results showed that the enhancement

[a]Graduate School of Bionics, Tokyo University of Technology, 1404-1 Katakura, Hachioji, Tokyo 192-0982, Japan. E-mail: yano@stf.teu.ac.jp

[b]School of Bioscience and Biotechnology, Tokyo University of Technology, 1404-1 Katakura, Hachioji, Tokyo 192-0982, Japan

[c]Graduate School of Computer Sciences, Tokyo University of Technology, 1404-1 Katakura, Hachioji, Tokyo 192-0982, Japan

effect was based on the interference phenomena and that the excitation light and fluorescence may be involved. Multilayered structures with Al_2O_3 as an optical interference material, instead of LiF or SiO_2,[16,17] have been applied to highly sensitive fluorescence measurements for DNA microarrays.[18]

We recently focused on a plasma polymerization technique for preparing a simple and excellent optical interference material alternative to SiO_2 or Al_2O_3. Plasma polymerization is a simple and attractive technique for depositing thin polymeric films on various substrate types in a dry process.[19,20] Plasma-polymerized films (PPFs) are unique because they are highly cross-linked, pinhole-free, and chemically stable. Plasma polymerization has been widely employed in bioanalytical applications, including the enhancement of cell adhesion and proliferation,[21–23] DNA arrays,[24,25] glucose biosensors,[26,27] and immunosensors.[28] We previously demonstrated that PPFs containing hexamethyldisiloxane (HMDS) as a monomer could be suitable optical interference layers for multilayered glass slides[29] and 96-well plastic microplates,[30] for fluorescence-based immunoassays, exhibiting 81- and 88-fold fluorescence enhancements, respectively.

An interesting feature of PPFs is that their surface characteristics can be easily controlled by adopting suitable organic monomers according to each strategy.[19] For example, allylamine is one of the most popular monomers for creating amino groups on substrate surfaces.[31] The introduction of amino groups to biochips is advantageous when the biochip surfaces are required to be hydrophilic.[21] In addition, the amino groups can be used to immobilize biomaterials, such as antibodies and enzymes, using chemical cross-linkers for covalent bonding or simply by physical adsorption. HMDS was suitable for the immobilization of antibodies when used as an optical interference layer because of its hydrophobicity, which is generally suitable for antibody immobilization.[29,30] The immobilization of biomaterials on substrates by covalent bonding is important for constructing robust biosensors and obtaining stable sensor signals for long periods without detachment from the sensor surfaces. PPF applications for the covalent immobilization of biomaterials have been reported by coupling hydrophilic functional-group-containing monomers and cross-linkers, such as ethylenediamine/glutaraldehyde,[32] acrylic acid/N-hydroxy succinimide (NHS)/1-ethyl-3-(3-dimethylaminopropyl) carbodiimide (EDC),[25] and cyclopropyl-amine/glutaraldehyde.[28]

This study fabricated multilayered glass slides by plasma polymerization using acetonitrile as a monomer. Acetonitrile can be used to introduce amino groups to the surface of PPFs although it lacks amino groups itself. Acetonitrile-derived PPFs have been characterized[33] and applied in glucose biosensors.[34] After the surface characterization and analyses of the capability of the glass slides for fluorescence enhancement, the modified glass slides were applied to aptamer-based sandwich assays by immobilizing aptamers on the PPFs through amino groups by cross-linking (Fig. 1). Thrombin was selected as a target molecule in the aptamer-based sandwich assays because two thrombin-specific aptamers, G15D[35] and 60-18[29],[36] have been well characterized among other targets and applied in many fluorescence-based biosensors,[37] including sandwich format[38] and label-free assay using DNA-templated gold nanoclusters
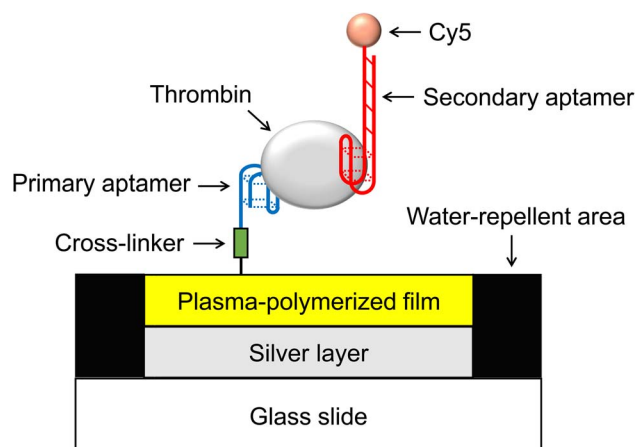

Fig. 1 Schematic representation of aptamer–based sandwich assay using multilayered glass slide.

and MnO_2 sheets.[39] This could be a suitable model assay to evaluate the efficacy of the proposed multilayered substrates.

First, we demonstrate that PPFs can serve as dual-function layers for the introduction of functional groups to immobilize biomaterials and optical interference materials to achieve fluorescence enhancement.

2. Experimental

2.1. Materials

Acetonitrile and human α-thrombin were purchased from Fujifilm Wako Pure Chemical Corp. (Osaka, Japan) and Haematologic Technologies, LLC (VT, USA), respectively. N-(6-maleimidocaproyloxy)sulfosuccinimide (Sulfo-EMCS) and chymotrypsin were purchased from Dojindo Laboratories (Kumamoto, Japan) and MP Biomedicals, LLC (OH, USA), respectively. Other reagents were of analytical grade and purchased from Fujifilm Wako Pure Chemical Corp. (Osaka, Japan). Standard (S1112, 76 × 26 mm^2) and 24-well water-repellent glass slides (TF2404, 76 × 26 mm^2) were purchased from Matsunami Glass Industries Ltd (Osaka, Japan). Oligonucleotides were purchased from Tsukuba Oligo Service Co., Ltd (Ibaraki, Japan). Oligo-Cy5,5′-TATTTCCCGGGAACCCA-Cy5-3′, comprising part of the cytochrome P450 sequence, was 17 nucleotides labeled with cyanine5 (Cy5) at the 3′ terminus. Oligo-Cy5-SH, 5′-Cy5-TGGGTTCCCGGGAAATA-SH-3′, had the complementary sequence of Oligo-Cy5 and was labeled with Cy5 at the 5′ terminus and a thiol group at the 3′ terminus. The primary aptamer for thrombin, 5′-GGTTGGTGTGGTTGGTT-SH-3′, was designed and synthesized based on the G15D sequence. It contained two thymines and three methylene groups at the 3′ terminus of the G15D sequence as spacers and was further labeled with a thiol group. The secondary aptamer, 5′-AGTCCGTGGTAGGGCAGGTTGGGGTGACT-Cy5-3′, was obtained by labeling the 3′ terminus of 60-18[29] with Cy5.

2.2. Deposition of metal layers

A 24-well water-repellent glass slide has a grid of 4 by 6 circular bare glass areas of ϕ 4.0 mm. The areas without wells are coated

with black water-repellent material such that all the reactions and measurements can be conducted in areas with the same size of glass. The glass slide was covered with a punched masking tape (3M Company, MN, USA) with the same size and position of holes as those of the reaction spots of the slide. Thereafter, it was cleaned by sonication in ethanol for 30 min, washed in ultrapure water, and dried. A chromium layer (as an adhesive) and a silver layer (as a metal mirror) were deposited successively onto the slides to prepare multilayer structures. Both layers were fabricated using a sputtering apparatus (CFS-4ES, Shibaura Mechatronics Corp., Kanagawa, Japan) with an output of 200 W, and the deposition times for chromium and silver were 15 s and 7 min, respectively. The deposition of metal layers on the standard glass slides was similarly conducted without the use of masking tapes.

2.3. Preparation of PPFs

A plasma deposition system (BP-1, Samco Inc., Kyoto, Japan) with two external electrodes horizontally set along the vacuum chamber 15 cm above the sample stage was used to prepare PPFs, as previously reported.[30] In addition, a radio frequency (RF) generator (RFG-300, Samco Inc., Kyoto, Japan) coupled to a matching box to minimize the reflected power, was employed. The working frequency of the power supply was 13.56 MHz.

A standard glass slide was placed on the sample stage of the plasma deposition apparatus. The chamber was evacuated, and a carrier gas of acetonitrile or other monomers was passed into the chamber at a constant flow rate of 20 cubic centimeters per minute (ccm). The background pressure was approximately 0.4 torr. The plasma was discharged at various RF powers to deposit PPFs on the glass slides. Several PPFs of different thicknesses were prepared by varying the deposition time. The deposition was analyzed using an ellipsometer (ESM-1T, ULVAC, Kanagawa, Japan) by measuring the thickness of the PPFs simultaneously formed on small reference silicon chips placed on the sample stage.

The PPF surfaces were analyzed using a Fourier transform infrared (FTIR) spectrometer (FT/IR-670Plus, Jasco International Co., Ltd, Tokyo, Japan) equipped with a reflection absorption spectroscopy attachment. The FTIR measurement was conducted under vacuum conditions by evacuating the sealed sample chamber using a rotary pump. The resolution of the wavenumber was determined to be 4 cm^{-1} using a HgCdTe (MCT) detector.

2.4. Influence of washing and RF power on PPF properties

Standard glass slides and silicon chips were coated with acetonitrile films by plasma polymerization for 5 min at an RF power of 100 W. They were washed in ultrapure water (10 mL) in a plastic incubation container (4 wells, $104 \times 169.5 \times 34.9$ mm^3, Ina Optika Co., Ltd, Osaka, Japan) for different times with mild agitation of *ca.* 60 rpm. using a shaker (MMS, Tokyo Rikakikai Co., Ltd, Tokyo, Japan) and dried at room temperature. The thickness and surface of the acetonitrile layer were analyzed by ellipsometry and FTIR spectroscopy, respectively. The relationships between deposition time and PPF thickness were evaluated using PPF-coated silicon chips prior to and after washing for different times. Similar analyses were conducted using PPF-coated glass slides prepared at various RF powers.

2.5. Fluorescence measurement of Oligo-Cy5 on multilayered glass slide with acetonitrile as a monomer

A multilayered structure was constructed on a standard glass slide at an RF power of 200 W using acetonitrile as a monomer for plasma polymerization for different deposition times. The substrates were washed with ultrapure water for 30 min with mild agitation and dried. Oligo-Cy5 was dissolved in sterilized ultrapure water and further diluted in phosphate-buffered saline (PBS; pH 7.4) to obtain 100 μM and 1 μM solutions, respectively. Thereafter, 2 μL each of the 1 μM DNA solution was spotted on six areas of the multilayered glass slide and dried. Afterward, 2D fluorescence images were obtained with a scanner (Pharos-FX, Bio-Rad, USA) using an excitation/ emission wavelength of 635/695 nm, and the fluorescence intensity was analyzed using the Quantity One Software (Bio-Rad). The fluorescence intensity from each spot was calculated by subtracting the background signal from the spot prepared under similar deposition conditions without sample loadings. The thickness of each PPF was measured using the ellipsometer by measuring the thickness of the PPFs simultaneously formed on small reference silicon chips placed on the same sample stage.

2.6. Immobilization of Oligo-Cy5-SH on multilayered glass slides prepared using nitrogen-containing monomers and comparison of fluorescence intensities

A multilayered structure was constructed on a 24-well water-repellent glass slide at an RF power of 200 W using acetonitrile or cyclopropylamine for 8 min and allylamine for 9 min. PPF-deposited substrates were also prepared in a similar manner using glass slides without silver layer as controls. Oligo-Cy5-SH was dissolved in sterilized ultrapure water and further diluted in PBS to obtain 100 μM and 2 μM solutions, respectively. Thereafter, it was heat-denatured at 95 °C for 5 min and immediately chilled on ice to allow the formation of a proper 3D structure. Sulfo-EMCS and tris(2-carboxyethyl)phosphine hydrochloride (TCEP) were dissolved in PBS to obtain 5 mM and 10 mM solutions, respectively.[40] The thiol group of Oligo-Cy5-SH was tethered to the maleimide group of Sulfo-EMCS with mild mixing for 30 min at room temperature in a mixture of 1 μM Oligo-Cy5-SH, 2 mM Sulfo-EMCS, and 0.1 mM TCEP in PBS. Thereafter, 15 μL each of the mixture was applied to the surface of four wells and incubated for 60 min at room temperature. This was performed to enable the immobilization of Sulfo-EMCS-tethered Oligo-Cy5-SH to the PPF *via* covalent bonding between the succinimide group of Sulfo-EMCS and the amino group of the PPF surface. After washing in PBS with mild mixing and drying, 2D fluorescence images were obtained using the scanner, and the fluorescence intensity was analyzed.

2.7. Aptamer sandwich assay for thrombin on multilayered glass slide

A multilayered structure for the fluorescence-based aptamer sandwich assay was similarly prepared on a 24-well water-repellent glass slide as described in Section 2.3 but with an

RF power of 200 W for 9 min. PPFs were also formed on small reference silicon chips simultaneously placed on the same sample stage to measure their PPF thickness using the ellipsometer.

The thiol-labeled primary aptamer for thrombin was dissolved in sterilized ultrapure water and further diluted in PBS to obtain 100 μM and 2 μM solutions, respectively. Thereafter, it was heat-denatured at 95 °C for 5 min and immediately chilled on ice to achieve a proper 3D structure. Sulfo-EMCS and TCEP were dissolved in PBS to obtain 5 mM and 10 mM solutions, respectively. The thiol group of the primary aptamer was tethered to the maleimide group of Sulfo-EMCS with mild mixing for 30 min at room temperature in a mixture of 1 μM primary aptamer, 2 mM Sulfo-EMCS, and 0.1 mM TCEP in PBS. Thereafter, 15 μL each of the mixture was applied to the surface of four wells and incubated for 60 min at room temperature. This was performed to enable the immobilization of the Sulfo-EMCS-tethered primary aptamer to the PPF *via* covalent bonding between the succinimide group of Sulfo-EMCS and the amino group of the surface of PPF.

The Cy5-labeled secondary aptamer was dissolved in sterilized ultrapure water and further diluted with a binding buffer [50 mM Tris–HCl (pH 8.0), 100 mM NaCl, 5 mM KCl] to obtain 100 μM and 2 μM solutions, respectively. Thereafter, it was heat-denatured at 95 °C for 5 min and immediately chilled on ice to achieve a proper 3D structure. The proteins and secondary aptamer were allowed to interact for 60 min at room temperature in a mixture of 1 μM thrombin or chymotrypsin as a control and 1 μM secondary aptamer in a binding buffer for 60 min at room temperature. This was performed with mild shaking. Protein-free samples were prepared as a negative control.

After washing the multilayered substrates immobilized with the primary aptamer by Sulfo-EMCS in a binding buffer, 15 μL each of the mixture of protein and the secondary aptamer was applied to the surfaces of four wells. Afterward, they were incubated for 60 min at room temperature to allow sandwich interaction. After washing with a binding buffer and drying, 2D fluorescence images were obtained. The fluorescence intensity from each well was calculated by subtracting the background signals from wells prepared under similar deposition conditions without sample loadings.

3. Results and discussion

3.1. Influence of washing of PPF on thickness

It is important to fabricate PPFs with the desired thickness to obtain the maximum fluorescence enhancement effect. The thickness of PPFs can be easily adjusted by changing the deposition time, and the thickness demonstrates a linear relationship with the deposition time.[30] Thus, a calibration curve is a suitable index for estimating the optimal deposition time to obtain optimal PPF thickness. However, in our preliminary attempt to perform the aptamer sandwich assay, we did not observe the fluorescence enhancement phenomena on the multilayered substrates (data not shown). We assumed that during the multiple aqueous steps on the PPFs, including incubation with aptamers and washing with buffers, the PPF

thickness might have decreased. Thus, the influence of the washing of PPFs on their thickness was examined.

After PPFs were deposited on silicon chips containing acetonitrile as a monomer for 5 min at an RF power of 100 W, they were washed using ultrapure water with mild agitation for different times and dried. The thickness of the PPFs prior to and after each washing was measured by ellipsometry. Fig. 2a shows the relationships between the washing times and PPF thickness. The PPF thickness decreased to approximately 53% only by washing for 10 min, whereas further washing only minimally influenced the thickness. Although plasma polymerization can
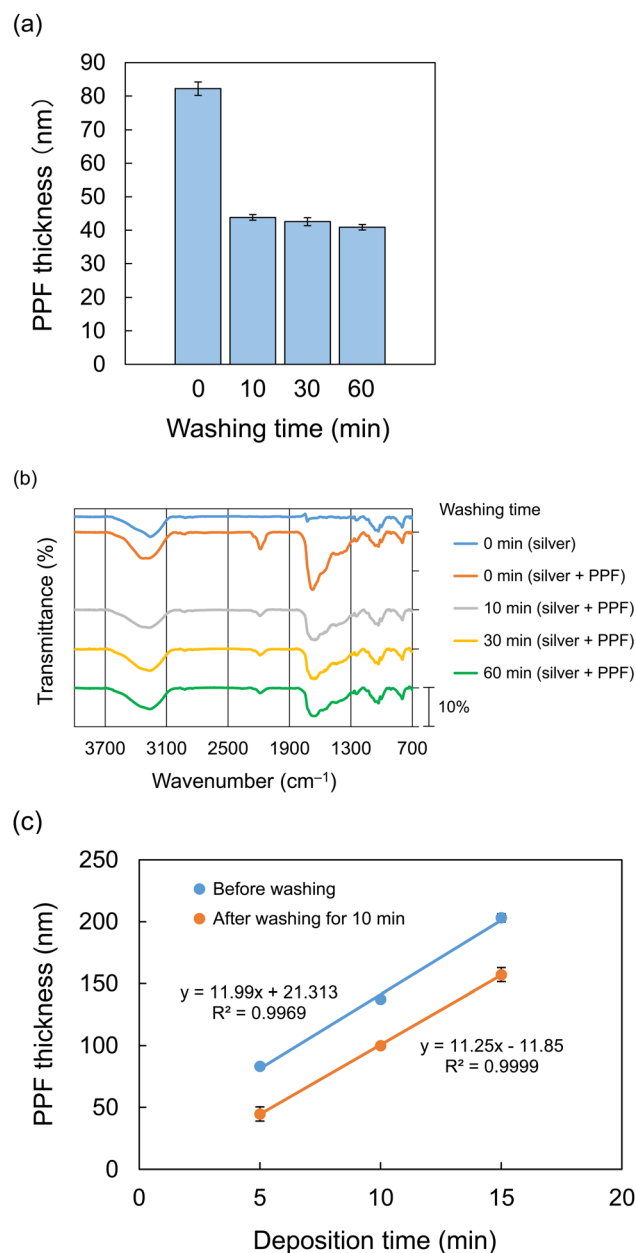

Fig. 2 Influence of washing of PPFs on (a) thickness, (b) FTIR spectra, and (c) the relationship between deposition time and PPF thickness. PPFs were deposited on silicon chips (a) and silver–coated glass slides (b). The error bars in (a) and (c) indicate the standard deviation of five measurements.

generally create a fine and stable polymer network, the results showed that PPF deposition using acetonitrile as a monomer under the aforementioned conditions might be insufficient to form a stable polymeric structure. Thus, the PPF surfaces prior to and after washing were further analyzed by FTIR spectroscopy.

After the glass slides were coated with a silver layer by sputtering, the PPFs were similarly deposited and washed as in Fig. 2a. The FTIR spectrum of the unwashed silver surface exhibited a broad band at 3250 cm^{-1} and weak peaks at 1050 and 800 cm^{-1} (Fig. 2b). These peaks were possibly due to the oxidized silver and the surface water condensed on the window of the liquid-N$_2$-chilled MCT detector. The oxidized silver bonds were considered to comprise Ag–O–H, Ag–O–Ag, Ag=O, etc.[41] The peak at 3250 cm^{-1} was assigned to the stretching vibration modes of the O–H bonds, and the weak peaks at 1050 and 800 cm^{-1} were attributable to the liberational motion and combinational vibration of molecular networks of water.[42] The multilayered slide exhibited a strong peak at approximately 1700 cm^{-1}, attributable to the stretching modes of the C=O bonds of primary and secondary amide, indicating the successful formation of a PPF with an amino group made of acetonitrile. The plasma products of organic materials are prone to contain carboxy groups,[43] which are expected to react with plasma-produced amino groups to form amide groups. The strong peak at approximately 1700 cm^{-1} was partially ascribed to unreacted carboxy groups. A broad peak around 3300 cm^{-1} comprised O–H bonds of surface water at 3250 cm^{-1} in addition to a new peak at 3325 cm^{-1} attributed to NH$_2$ symmetric and antisymmetric stretching vibration of the plasma-produced amino group. The plasma-derived amino group supports a possible plasma polymerization phenomenon using acetonitrile without an amino group. However, a small peak around 2200 cm^{-1} attributed to C≡N nitrile stretching indicated that some of the original moieties of the monomer were incorporated into the polymer network. Interestingly, by washing in pure water for 10 min, the three characteristic peaks significantly decreased, and further washing for over 10 min did not affect the absorbance spectra. These results were consistent with those shown in Fig. 2a. A transmittance peak of the multilayered substrate at 1677 cm^{-1} after washing for 10 min decreased to approximately 49% compared with that of the unwashed PPF, which was comparable to that shown in Fig. 2a.

Next, we examined the influences of washing for 10 min on the PPF thickness for various deposition times. The thickness was proportional to the deposition time prior to and after washing (Fig. 2c). The differences between the thicknesses prior to and after washing were practically identical under the three deposition time conditions. This indicates that plasma polymerization for any deposition time forms unstable and washable structures on their surfaces but that their thickness may be practically the same, regardless of the deposition time.

Fang et al. immersed nanocomposites prepared by plasma polymerization using 4-vinyl pyridine as a monomer in PBS solution overnight to remove unbound monomer molecules or oligomers in the polymeric network.[44] Although the monomer, apparatus, and conditions for plasma polymerization differed,

the surfaces of the present PPFs might have been similarly covered with unbound acetonitrile monomer molecules and oligomers, as well as those formed using 4-vinyl pyridine. A 10 min wash was shown to be sufficient for acetonitrile PPFs, whereas Fang washed nanocomposites overnight to remove an unstable surface layer, which might be dependent on monomers and polymerization conditions. These findings show that to obtain PPFs with optimal thicknesses for fluorescence enhancement, the deposition time should be set considering the decrease in thickness after washing, as shown in Fig. 2c.

3.2. Influence of RF power on PPF properties

Fig. 2 shows that experimental protocols, including the incubations of multilayered substrates in aqueous solutions containing aptamers, target molecules, or buffers, may significantly affect PPF thickness. An alternative solution to easily obtaining PPFs with optimal thicknesses rather than by controlling deposition time is to explore other polymerization conditions that afford a less unstable surface layer. Thus, we examined the effect of RF power during polymerization on changes in thickness. PPFs were prepared on silicon chips at various RF powers for 10 min, and the thickness of each PPF prior to and after washing for 30 min was measured. Fig. 3 shows that the properties of PPFs were considerably dependent on the powers of plasma polymerization. At the same deposition time, the thickness of the unwashed PPFs decreased with an increase in the RF power. Subsequent washing led to a decrease in the thickness of all the four PPFs. However, the decrease ratios reduced as the RF powers increased. The thickness of the PPF prepared at 50 W decreased to 41% after washing, whereas the ratio of that obtained at 200 W was 76%. These results showed that the PPF thicknesses prior to and after washing correlated with the RF power.

The influence of the RF power on the surface properties of the PPFs was further analyzed by FTIR spectroscopy. After glass slides were coated with silver by sputtering, acetonitrile PPFs were deposited at various RF powers for 10 min. Their surfaces
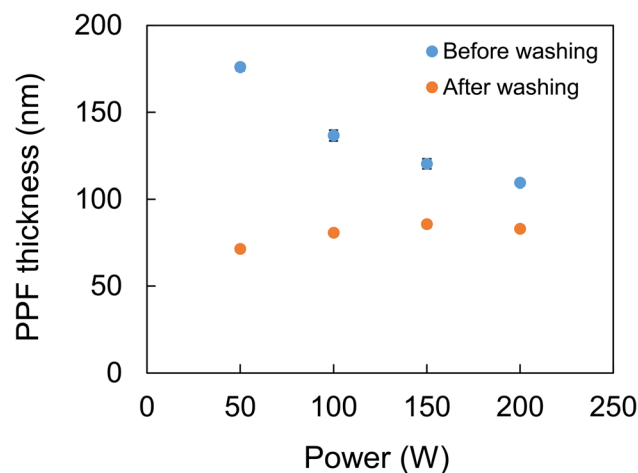

Fig. 3 Influence of RF power on PPF thickness. The error bars indicate the standard deviation of five measurements.

were examined and compared prior to and after washing for 30 min with ultrapure water by FTIR spectroscopy. Prior to washing (Fig. 4a), characteristic transmittance peaks (*e.g.*, around 1700 and 3300 cm^{-1}) similar to those shown in Fig. 2b, were observed for all the PPFs prepared at various powers, although the peak heights decreased as the power increased. After washing, the peaks obtained with PPFs at 50, 100, and 150 W significantly decreased; however, a minimal change in the transmittance peak was observed at 200 W (Fig. 4b). The peak of a PPF at 1677 cm^{-1} prepared at 50 W decreased to 50% after washing, whereas the ratio of that obtained at 200 W was 105%. The numerical decrease ratios obtained from Fig. 3 and 4 at 50 and 200 W slightly differed, respectively. However, the results showed that the change in PPF thickness caused by washing could be minimized at an output of 200 W. Furthermore, it showed that PPF deposition could be easily adjusted in terms of the optimal thickness, which is important for maximum fluorescence enhancement.

As shown in Fig. 4a, a relatively weak peak around 2200 cm^{-1} attributed to C≡N nitrile stretching, possibly originating from the moiety of the monomer, was observed but decreased with an increase in the RF power. Similarly, the deposition rate decreased as the RF power increased (Fig. 3). Considering these phenomena, we suggest that when the RF power is low, the degree of fragmentation and recross-linking by polymerization might be low and, therefore, susceptible to washing, resulting in a decrease in thickness. Oppositely, an RF power as high as 200 W might promote a complicated polymer network and decrease unreacted monomers or oligomer networks on PPF surfaces.

3.3. Enhancement of fluorescence intensity from Oligo-Cy5 on multilayered substrate

Considering the principle of fluorescence enhancement in this study based on the optical interference at the dielectric layer on the PPF, it is imperative to prepare PPFs with optimal thicknesses for assays. Thus, the relationship between PPF thickness after washing and the fluorescence intensity was examined to obtain the optimal thickness. Oligo-Cy5, a single-stranded oligonucleotide labeled with fluorophores, was used to evaluate the efficacy of fluorescence enhancement on various PPFs without immobilization steps or complex interactions between complementary strands or target molecules. The surfaces of standard glass slides were coated with a silver layer and subsequently modified with acetonitrile PPFs at an RF power of 200 W for various deposition times. After washing with ultrapure water for 30 min, the Oligo-Cy5 solution was spotted on six areas, and 2D fluorescence images were obtained.

The images revealed that Cy5 fluorescence was highly enhanced on the multilayered substrates compared with that observed from the chip without PPF (Fig. 5). The degree of enhancement was dependent on the PPF thickness; the maximum fluorescence intensity was obtained from an 84 nm-thick PPF layer after washing, indicating 11- and 281-fold enhancements of fluorescence compared with those obtained from the substrates with a bare surface and only modified by a silver layer, respectively. The deposition time to obtain an 84 nm-thick PPF layer after washing was 8 min.

A correlation was observed between the thickness of an interference layer (Al$_2$O$_3$) and the fluorescence intensity using various fluorophores.[45] In particular, the fluorescence intensity of Cy5 was most enhanced when the Al$_2$O$_3$ thickness was 104 nm in the range of 0–200 nm. In this case, the Cy5 molecule solution was spotted using a spotting machine, whereas the Cy5-labeled DNA solution was manually spotted in our study. This indicated that the bulky moiety of Oligo-Cy5 comprising 17 nucleotides and the substantial DNA layer might have affected the optimal thickness condition. Conversely, in our previous study, the Cy3-labeled antibody solution was spotted on multilayered substrates containing HMDS as a monomer, and the maximum fluorescence intensity was obtained from a 63 nm-thick PPF layer.[29] As the excitation wavelength of Cy5 (635 nm) is longer than that of Cy3 (532 nm), a thicker layer for the fluorescence enhancement of Cy5 than that for Cy3 might make sense considering the optical interference.

3.4. Influence of monomers on fluorescence enhancement using immobilized Oligo-Cy5-SH

The formation of amino groups on PPF surfaces is vital for the robust immobilization of aptamers using appropriate cross-linkers. Apart from acetonitrile, certain organic compounds containing amino groups have been utilized to fabricate hydrophilic PPFs, including allylamine[31] and cyclopropylamine.[28] PPFs with surface amino groups can be easily prepared
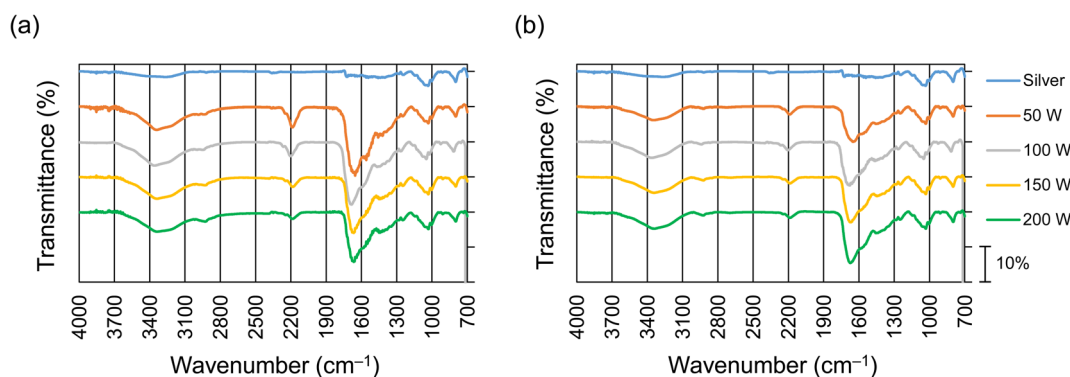

Fig. 4 Influence of RF power on FTIR spectra (a) prior to and (b) after washing.
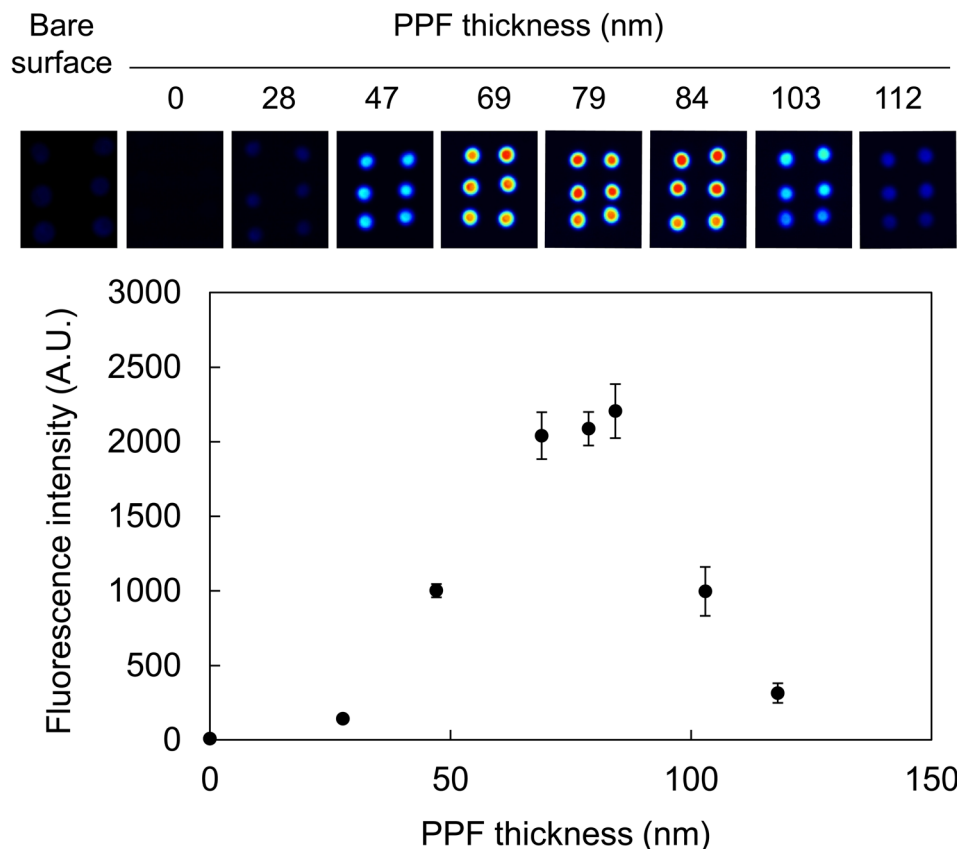
Fig. 5 Enhancement of fluorescence intensity from Oligo–Cy5 on multilayered substrate. All the substrates, except one with a bare surface, were coated with silver layers prior to plasma polymerization. The error bars indicate the standard deviation of six measurements.

using such amino group-containing organic monomers. Thus, to widen the variety of PPFs with various characteristics, allylamine, cyclopropylamine, and acetonitrile were utilized as monomers for plasma polymerization, and the resulting PPFs were evaluated to determine if they could serve as functional biochips for fluorescence enhancement.

The surfaces of 24-well water-repellent glass slides were coated with a silver layer and subsequently modified by plasma polymerization at an RF power of 200 W using acetonitrile or cyclopropylamine for 8 min and allylamine for 9 min. Each deposition time was set such that the thickness of each PPF after washing with ultrapure water for 30 min was approximately in the range of 70–90 nm. Oligo-Cy5-SH modified with fluorophores and a thiol group was used to evaluate the efficacy of the immobilization and fluorescence enhancement on the PPFs before performing a complex aptamer sandwich assay. After the Oligo-Cy5-SH solution was incubated with Sulfo-EMCS and TCEP in PBS to be tethered to the maleimide group of Sulfo-EMCS, the mixture was applied to the surface of the wells to impart immobilization to the PPFs.

Fluorescence analyses revealed that the substrates only modified with acetonitrile, allylamine, or cyclopropylamine by plasma polymerization exhibited very low fluorescence intensities, similar to those obtained with the substrate with a bare surface (Fig. 6). However, the fluorescence of multilayered substrates modified with silver and any PPF was enhanced. The

highest intensity was obtained from the PPF modified with silver and acetonitrile (approximately 19-fold enhancement compared with that obtained from the substrate only modified with acetonitrile). We selected cyclopropylamine and allylamine as alternative monomers because they contained amino groups, through which PPFs with amino groups necessary for the immobilization of DNA might be easily obtained. Fig. 6 suggests that the present conditions of plasma polymerization (RF power of 200 W) might have been rather severe for those two monomers and probably degraded amino groups, resulting in fewer functional groups on the surfaces. The difference in the refractive indices or other chemical and/or physical properties of PPFs might also affect fluorescence enhancement. Nevertheless, as 5- and 12-fold enhancements were observed from the multilayered substrates prepared using allylamine and cyclopropylamine, respectively, it is possible to utilize these monomers after determining the optimal polymerization conditions.

3.5. Aptamer sandwich assay for thrombin on multilayered glass slide

As the multilayered structure modified with PPFs using acetonitrile was shown to be advantageous for fluorescence enhancement, it was further utilized for an aptamer sandwich assay, and its efficacy for the sensitive detection of a target molecule was examined. A multilayered structure was prepared on a 24-well water-repellent glass slide and washed. After the
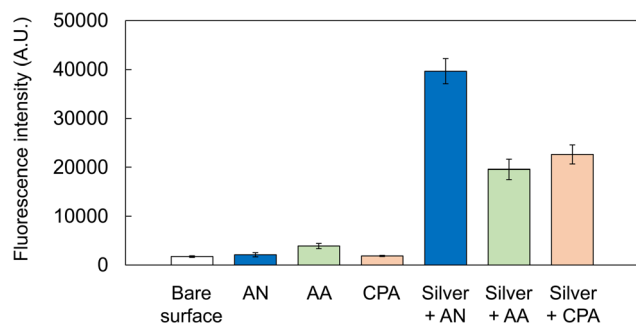
Fig. 6 Influence of monomers (acetonitrile (AN), allylamine (AA), and cyclopropylamine (CPA)) on fluorescence enhancement using immobilized Oligo-Cy5-SH. The error bars indicate the standard deviation of four measurements.

thiol group of the primary aptamer for thrombin was tethered to the maleimide group of Sulfo-EMCS, the mixture was applied to the surface of wells and incubated to impart immobilization to the PPF *via* covalent bonding between the succinimide group of Sulfo-EMCS and the amino group of the PPF surface. The pre-incubated mixture of the Cy5-labeled secondary aptamer and 1 µM protein was applied to the surfaces of the wells and allowed to interact with the immobilized primary aptamer. Afterward, a 2D fluorescence image was obtained. The highest fluorescence intensity was obtained when the multilayered substrate was used against thrombin, exhibiting approximately 5.1-fold enhancement compared with that obtained from the substrate with a bare surface using thrombin (Fig. 7). The fluorescence intensities from the substrates only modified with PPF targeting thrombin and the multilayered substrates with no protein or targeting chymotrypsin were the same, comparable to that obtained from the substrate with a bare surface targeting thrombin. These results suggest that the multilayered structure modified with PPF could be successfully applied to the aptamer-based sandwich assay and enhance the fluorescence intensity with specificity. A high fluorescence signal was obtained with the substrate only modified with a silver layer targeting thrombin. This might have been because the Cy5-labeled

secondary aptamer was physically adsorbed to the silver surface, and its nonspecific fluorescence signal was enhanced to an extent by the mirror effect of the silver surface. However, Fig. 7 shows that such a nonspecific signal can be avoided by immobilizing the primary aptamer and performing the sandwich assay on the surface of the multilayered substrates.

The selectivity of our fluorescence enhancement system depends not only on specificity of the thrombin aptamers but also on hydrophilicity of PPFs. We employed acetonitrile PPF, which presents amino groups on its surface. During the aptamer-based sandwich assay, PPFs are immersed in the binding buffer (pH 8.0), and the remaining amino groups that are not used for immobilization of the primary aptamer may be protonated. Analyte molecules with a negative charge may bind to the surface of the substrates with positive charge of ammonium cations. At first, we expected the nonspecific binding of Cy5-labeled secondary aptamer to the PPFs because of its negative charge. However, Fig. 7 shows that the fluorescence intensities in the condition of PPF + thrombin remained only slightly increased compared with that of bare surface + thrombin. This might indicate only limited binding of Cy5-labeled secondary aptamer to the surface, suggesting that most amino groups created by plasma polymerization were used for immobilization of the primary aptamer. We used thrombin (pI 7.0) and chymotrypsin (pI 8.8) as a control to examine the specificity of our system. In the binding buffer (pH 8.0) thrombin and chymotrypsin have negative and slightly positive charges, respectively. However, as mentioned above, the charge of the proteins may not affect the nonspecific binding to the PPFs with little remaining amino groups. Possible interfering substances may include albumin, transferrin and IgG, and their pI are 5–6, 5–6 and 6–9, respectively. Only limited nonspecific binding of these proteins could be expected for the same reason.

A calibration curve was obtained using the multilayered substrate against various thrombin concentrations. Fig. 8 shows that the fluorescence intensity correlated with thrombin
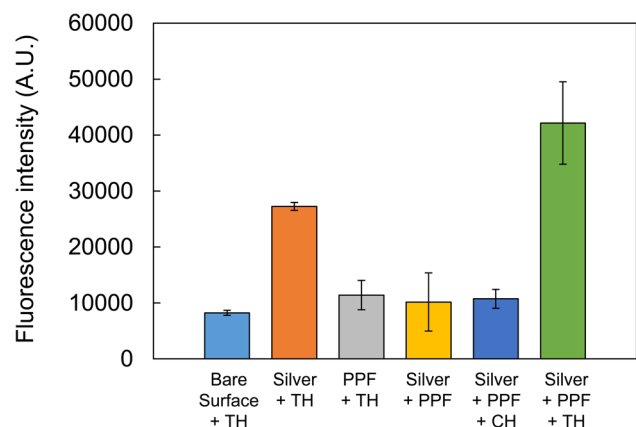

Fig. 7 Aptamer sandwich assay for thrombin (TH) on multilayered glass slide. Chymotrypsin (CH) was used as a control. The error bars indicate the standard deviation of four measurements.
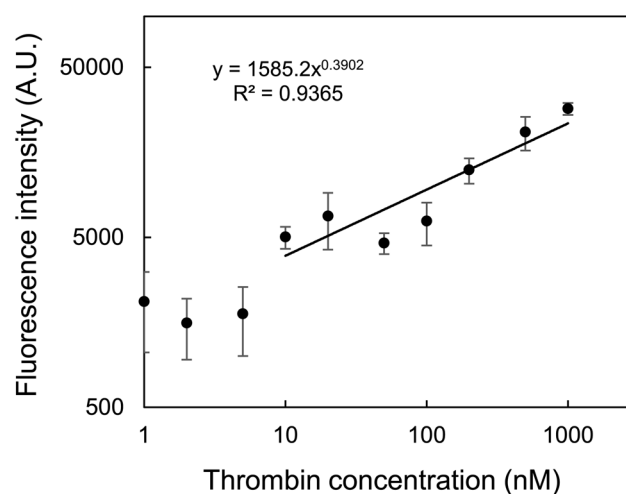

Fig. 8 Calibration curve of fluorescence intensity as a function of thrombin concentration. The error bars indicate the standard deviation of four measurements.

Table 1 The comparison of different fluorescence methods for thrombin detection

Analytical method	Linear range (nM)	LOD (nM)	References
DNA-gold nanoclusters and MnO_2 sheets	0.2–20	0.1	39
Stimulus-response click chemistry	14–285	8.1	46
Aptamer bio-dots and gold nanoparticles	8–160	7.4	47
FRET between CdS quantum dots and gold nanoparticles	1.35–54.0	0.38	48
Plasma polymerization	10–1000	2.8	This work

concentration in the range of 10–1000 nM. Based on the 3σ rule (S/N = 3), LOD was calculated to be 2.8 nM. Fig. 7 shows that even 1 μM thrombin could not be detected by any substrate with a bare surface or only modified with PPF. Thus, the effect of the multilayered structure could contribute at least a 200-fold enhancement of the LOD. Fig. 8 does not always indicate a perfect linear relationship, and this may be due to inaccurate taping of a punched masking tape as described in Section 2.2, causing slight changes in the positions of the circular reaction area. This may be overcome by using microplates with uniform bottom areas for the alternative assay format as in our previous study.[30] Nevertheless, we are confident that in this study we could first demonstrate the new methodology for applying PPFs to aptamer-based sandwich assay for fluorescence enhancement. Linearity may also be improved by masking small amount of remaining amino groups using appropriate amidating reagents, or by simply increasing the salt concentration in the binding buffer to avoid nonspecific binding.

The linear range and LOD in this work are almost comparable or slightly inferior to those in other studies (Table 1). However, those performances may be improved by changing assay formats or buffer conditions. It is also clear that our method is cost-effective than using gold nanoparticles. More importantly, our method is not the homogeneous assay in the aqueous solution but is based on the molecular recognition on the aptamer-immobilized substrates. One advantage of plasma polymerization is its ability to facilitate batch PPF formation over large areas of assay formats, such as glass slides sized 76 × 26 mm² as used in this study, or even 96-well microplates.[30] The advantage can be utilized especially in DNA or antibody microarrays for high throughput analyses in the future.

4. Conclusions

This study demonstrated the potential of PPFs for fluorescence enhancement in aptamer-based sandwich assays. One of the important aspects of plasma polymerization is that the surface characteristics of PPFs can be easily controlled by selecting suitable organic monomers according to each strategy. We selected acetonitrile as a monomer to create an amino group on the surface of PPFs, enabling the successful robust immobilization of DNA aptamers by covalent bonding *via* the crosslinker, Sulfo-EMCS. To the best of our knowledge, this is the first study to assign two roles to PPFs: (i) introduction of functional groups to immobilize biomaterials and (ii) optical interference materials for fluorescence enhancement. The resulting multilayered glass substrates comprising a silver layer and PPFs

with dual functions could serve as an aptamer-based sandwich assay platform, achieving 5.1-fold fluorescence enhancement against thrombin. This study also revealed the basic surface characteristics of PPFs by FTIR in terms of the influence of washing on the decrease ratio of the amino group of PPFs. Although the physical properties of PPFs differ according to each plasma polymerization apparatus, the study findings are valuable, particularly for PPF applications for wet experiments. Considering that we have described the use of PPFs on 96-well microplates for a sandwich immunoassay, this study will be applied to more versatile 96-well microplates or even microfluidics made of polydimethylsiloxane (PDMS) for microanalysis.

Data availability

The data are available on request from the authors.

Author contributions

K. Y.: conceptualization, methodology, validation, formal analysis, resources, writing—original draft preparation, visualization, supervision, project administration and funding acquisition. Y. M.: methodology, validation, formal analysis, investigation, data curation and visualization. A. S.: formal analysis, investigation and data curation. M. O.: writing—review and editing and supervision. T. A.: writing—review and editing and supervision. I. S.: writing—review and editing and supervision.

Conflicts of interest

The authors declare no conflict of interest.

Acknowledgements

References

1 C.-H. Sang, S.-J. Chou, F. M. Pan and J.-T. Sheu, *Biosens. Bioelectron.*, 2016, **75**, 285–292.
2 C. Chen, J. Zhao, Y. Lu, J. Sun and X. Yang, *Anal. Chem.*, 2018, **90**, 3505–3511.
3 Q. Chen, T. Tian, E. Xiong, P. Wang and X. Zhou, *Anal. Chem.*, 2020, **92**, 573–577.

4 L.-G. Chen, J. Li, L. Sun and H.-B. Wang, *Talanta*, 2024, **271**, 125703.

5 S. M. Fothergill, C. Joyce and F. Xie, *Nanoscale*, 2018, **10**, 20914–20929.

6 D. Semeniak, D. F. Cruz, A. Chilkoti and M. H. Mikkelsen, *Adv. Mater.*, 2022, 2107986.

7 Y. Zhang, G. L. Keegan, O. Stranik, M. E. Brennan-Fournet and C. McDonagh, *J. Nanopart. Res.*, 2015, **17**, 326–337.

8 H. Li, M. Wang, W. Qiang, H. Hu, W. Li and D. Xu, *Analyst*, 2014, **139**, 1653–1660.

9 K. Dhanasiwawong, K. Thamaphat, M. Horprathum, A. Klamchuen, A. Phetsahai and P. Limsuwan, *Processes*, 2022, **10**, 202.

10 N. Momenbeitollahi, J. van der Zalm, A. Chen and H. Li, *Anal. Chim. Acta*, 2022, **1195**, 339443.

11 J.-H. Hwang, S. Park, J. Son, J. W. Park and J.-M. Nam, *Nano Lett.*, 2021, **21**, 2132–2140.

12 W. R. Holland and D. G. Hall, *Opt. Lett.*, 1985, **10**, 414–416.

13 K. G. Sullivan, O. King, C. Sigg and D. G. Hall, *Appl. Opt.*, 1994, **33**, 2447–2454.

14 K. G. Sullivan and D. G. Hall, *J. Opt. Soc. Am. B*, 1997, **14**, 1149–1159.

15 K. G. Sullivan and D. G. Hall, *J. Opt. Soc. Am. B*, 1997, **14**, 1160–1166.

16 V. Marino, C. Galati and C. Arnone, *J. Biomed. Opt.*, 2008, **13**, 054060.

17 H. M. Hiep, H. Yoshikawa, M. Saito and E. Tamiya, *ACS Nano*, 2009, **3**, 446–452.

18 M. Yasuda and T. Akimoto, *Sens. Mater.*, 2018, **30**, 59–66.

19 H. Muguruma, *Plasma Processes Polym.*, 2010, **7**, 151–162.

20 J. Carneiro de Oliveira, M. de Meireles Brioude, A. Airoudj, F. Bally-Le Gall and V. Roucoules, *Mater. Today Chem.*, 2022, **23**, 100646.

21 P. Qi, W. Yan, Y. Yang, Y. Li, Y. Fan, J. Chen, Z. Yang, Q. Tu and N. Huang, *Colloids Surf., B*, 2015, **126**, 70–79.

22 B. Akhavan, S. Bakhshandeh, H. Najafi-Ashtiani, A. C. Fluit, E. Boel, C. Vogely, B. C. H. van der Wal, A. A. Zadpoor, H. Weinans, W. E. Hennink, M. M. Bilek and S. A. Yavari, *J. Mater. Chem. B*, 2018, **6**, 5845–5853.

23 H.-Y. Kim, B.-H. Kim and M.-S. Kim, *Materials*, 2022, **15**, 366.

24 H. Miyachi, K. Ikebukuro, K. Yano, H. Aburatani and I. Karube, *Biosens. Bioelectron.*, 2004, **20**, 184–189.

25 R. Jafari, F. Arefi-Khonsari, M. Tatoulian, D. Le Clerre, L. Talini and F. Richard, *Thin Solid Films*, 2009, **517**, 5763–5768.

26 K. Kojima, A. Hiratsuka, H. Suzuki, K. Yano, K. Ikebukuro and I. Karube, *Anal. Chem.*, 2003, **75**, 1116–1122.

27 H. Muguruma, T. Hoshino and Y. Matsui, *ACS Appl. Mater. Interfaces*, 2011, **3**, 2445–2450.

28 A. Manakhov, E. Makhneva, P. Skládal, D. Nečas, J. Čechale, L. Kalina, M. Eliáš and L. Zajíčková, *Appl. Surf. Sci.*, 2016, **360**, 28–36.

29 K. Yano, K. Yamano, A. Iwasaki, T. Akimoto, H. Miyachi and A. Hiratsuka, *Sens. Mater.*, 2015, **27**, 859–869.

30 K. Yano and A. Iwasaki, *Sensors*, 2017, **17**, 37.

31 Q. Chen, R. Förch and W. Knoll, *Chem. Mater.*, 2004, **16**, 614–620.

32 R. Nakamura, H. Muguruma, K. Ikebukuro, S. Sasaki, R. Nagata, I. Karube and H. Pedersen, *Anal. Chem.*, 1997, **69**, 4649–4652.

33 A. Hiratsuka, H. Muguruma, R. Nagata, R. Nakamura, K. Sato, S. Uchiyama and I. Karube, *J. Membr. Sci.*, 2000, **175**, 25–34.

34 H. Muguruma, A. Hiratsuka and I. Karube, *Anal. Chem.*, 2000, **72**, 2671–2675.

35 L. C. Bock, L. C. Griffin, J. A. Latham, E. H. Vermaas and J. J. Toole, *Nature*, 1992, **355**, 564–566.

36 D. M. Tasset, M. F. Kubik and W. Steiner, *J. Mol. Biol.*, 1997, **272**, 688–698.

37 H. Sun, N. Wang, L. Zhang, H. Meng and Z. Li, *Chemosensors*, 2022, **10**, 255.

38 Y. Wang, H. Li and D. Xu, *Anal. Chim. Acta*, 2016, **905**, 149–155.

39 H.-B. Wang, Y. Li, H.-Y. Bai and Y.-M. Liu, *Sens. Actuators, B*, 2018, **259**, 204–210.

40 C. Bayraç, F. Eyidoğan and H. A. Öktem, *Biosens. Bioelectron.*, 2017, **98**, 22–28.

41 W. M. Shume, H. C. A. Murthy and E. A. Zereffa, *J. Chem.*, 2020, 5039479.

42 L. Liu, J. Yang, X. C. Zeng, S. S. Xantheas, K. Yagi and X. He, *Nat. Commun.*, 2021, **12**, 6141.

43 K. S. Siow, L. Britcher, S. Kumar and H. J. Griesser, *Plasma Processes Polym.*, 2006, **3**, 392–418.

44 S. Fang, X. Dong, S. Liu, D. Penng, L. He, M. Wang, G. Fu, X. Feng and Z. Zhang, *Electrochim. Acta*, 2016, **212**, 1–9.

45 T. Akimoto and M. Yasuda, *Appl. Opt.*, 2010, **49**, 80–85.

46 Z. Chen, M. Sun, F. Luo, K. Xu, Z. Lin and L. Zhang, *Talanta*, 2018, **178**, 563–568.

47 L. Kuang, S.-P. Cao, L. Zhang, Q.-H. Li, Z.-C. Liu, R.-P. Liang and J.-D. Qiu, *Biosens. Bioelectron.*, 2016, **85**, 798–806.

48 P. Li, C. Luo, X. Chen and C. Huang, *RSC Adv.*, 2022, **12**, 35763–35769.